Catalysis
Science &
Technology

Accepted Manuscript

ROYAL SOCIETY
OF **CHEMISTRY**

www.rsc.org/catalysis

Journal Name

ARTICLE

Supported ionic-liquid-phase-stabilized Au(III) catalyst for acetylene hydrochlorination

Received 00th January 20xx,
Accepted 00th January 20xx

DOI: 10.1039/x0xx00000x

www.rsc.org/

Jia Zhao,[a, b] Shanchuan Gu,[a] Xiaolong Xu,[a] Tongtong Zhang,[a] Yi Yu,[a] Xiaoxia Di,[a] Jun NI,[a] Zhiyan Pan[b] and Xiaonian Li[a †]

Using high-valent Au(III) catalysis is highly desirable in many reactions, however it is plagued by the poor stability of Au(III) complexes. Still, conventional catalysts use only a small fraction of the Au content makes the high price and demand for Au is one of the major obstacles limiting their large-scale application. Here we demonstrate that stable and catalytically active Au(III) complexes can be obtained using Supported Ionic Liquid Phase (SILP) technology. The resulting heterogeneous Au–IL/AC catalysts combine the advantages of the catalytic species being stabilised in the Au(III) form by forming a Au(III)–IL complex and the need for less expensive metal catalyst because the active component can be better developed in a homogeneous reaction medium. When used in the acetylene hydrochlorination reaction, this catalyst displayed an excellent specific activity and superior long-term stability. Under the same reaction conditions, the Au(III)–IL/AC catalyst shows higher activity and stability towards vinyl chloride monomer (VCM) than IL-free Au/AC (C_2H_2 conversion = 72.1% at 180 °C compared to 16.1% without IL). It also delivered stable performance within the conversion of acetylene, reaching more than 99.4%, and there was only 3.7% C_2H_2 conversion loss after running for 300 h under the reaction conditions of a temperature of 180 °C and a C_2H_2 hourly space velocity of 30 h^{-1}. Its exceptional ability to maintain the high activity and stability further demonstrated the potential for the replacement of Hg-based catalysts for acetylene hydrochlorination.

Introduction

Polyvinyl chloride is not only one of the five general synthetic resins, but is also an important product for the sustainable development of the chlor-alkali industry. Current industrial production of the vinyl chloride monomer (VCM) uses the oxychlorination reaction of ethylene or direct hydrochlorination of acetylene.[1] Over the past decade, the manufacture of VCM based on acetylene has become increasingly competitive because of the lower cost of the coal-based process than the petroleum-based process.[2] However, the former synthesis in the presence of mercuric chloride catalysts is not a green process because of the volatility of the toxic $HgCl_2$ component, which can disperse into the environment and be a threat to human health.[3] Thus, hydrochlorination of acetylene using less hazardous mercuric-free catalysts is highly desirable to satisfy stringent environmental regulations.

Numerous efforts have been made to develop novel green catalysts for the efficient and sustainable hydrochlorination of acetylene. Although the pioneering work carried out by Hutchings and co-workers showed that Au(III) catalysts are the most promising materials for the hydrochlorination of acetylene because of their intrinsically high activity.[4,5] However, Au(III) catalysts commonly undergo significant deactivation owing to the facile reduction of Au(III) to Au(0) in the presence of electron-rich substrates because of the intrinsically highly positive standard redox potential of Au(III) (Au^{3+}/Au^0 = 1.52 V).[6-8] Thus, modalities that can enhance Au(III) stability are extremely important for practical applications. Additionally, current state-of-the-art hydrochlorination catalysts use Au or Au-based catalysts with a high content of Au (typically 1.0 wt%) to maintain their high activity, which makes the catalysts too expensive for widespread mass production of affordable VCM.[9-19] However, this is still a small fraction of the Au^{3+} content that is active in the reaction.[2,6,9] Although replacement of gold by less expensive materials can overcome this limitation, both low-cost non-precious metal (*e.g.*, $BiCl_3$)[20-22] and non-metal (*e.g.*, N-doped carbon materials) catalysts[23-25] suffer from the disadvantages of low conversion efficiency and fast deactivation, leading to these catalysts not being able to compete with their expensive counterparts. Thus, Au-catalyzed hydrochlorination is still recognized as the most promising acetylene hydrochlorination reaction. The goal of reducing the demand for Au is a major driving force in Au catalysis research. Using gold as efficiently as possible is a promising strategy. In this case, the most important parameter is dispersion. However, supported Au catalysts are nearly unavoidable to prevent the most of cationic gold species from reduction and

---

[a] Industrial Catalysis Institute of Zhejiang University of Technology, State Key Laboratory Breeding Base of Green Chemistry-Synthesis Technology, Hangzhou, 310014, P.R. China.

[b] Department of Environmental Engineering, Zhejiang University of Technology, Hangzhou, 310014, P.R. China.

[†] Tel: +86 571 88320002. E-mail address: xnli@zjut.edu.cn

aggregating in the Au-sol immobilization method, which is the most appropriate technique to obtain carbon-supported Au catalysts.

For hydrochlorination of acetylene, obtaining high active and stable catalysts requires proper catalyst design. Very recently, Hutchings and co-workers reported an inspiring sulfur-containing ligands stabilized Au(I) catalyst for acetylene hydrochlorination.[26] They showed that effectively the stability of gold-sulfur bonds is exploited in this methodology to prepare a stable cationic gold catalyst that is highly dispersed. The significantly greater hydrochlorination activity of these complexes can reduce the Au loading down to 0.1 wt% while maintaining comparable hydrochlorination activity (Au/C readily gives 100% conversion at 500 h^{-1} GHSV based on the total volume of reactant gas passed per volume of catalyst per hour). This high performance of these gold-sulfur complexes catalysts was attributed to the greater stability of these complexes to disperse and stabilize the cationic Au species during preparation and use.

Since highly efficient catalytic systems are always desirable, it is necessary to find new approaches of catalyst promotion. In this regard, we searched for a route to obtain stable catalytically active Au(III) complexes and enhance noble metal efficiency by supported ionic liquid (IL) phase (SILP) catalysis technology, which has recently been introduced for several liquid- and gas-phase reaction systems.[27-38] In these SILP systems, a thin IL film creates a uniform solvent environment for the dissolved transition-metal complex, while the highly porous solid on which this ionic catalyst solution is supported creates a large gas–liquid interfacial area for fast mass transport. These catalysts combine the advantages of the catalytic species being stabilized in the cationic form by forming a Au(III)–IL complex and the need for smaller amounts of expensive metal catalyst because the active component can be better developed in a homogeneous reaction medium to maintain its high activity. In addition, the negligible vapour pressure, large liquid range, and thermal stability of ILs ensure that the solvent is retained on the support in its fluid state even at elevated temperatures,[39] which makes SILP catalysts highly suitable for continuous processes.[33-35] More importantly, ILs are capable of stabilizing the highly oxidising metal and preventing the formation of agglomerates and dimmers.[40,41] All of these reasons indicate that the supported Au(III)–IL phase is a good candidate as a catalyst in the hydrochlorination of acetylene.

In this paper, we report the first use of a Au(III)–IL molecular catalyst system in which the catalyst remains active, selective, and stable over an extended period of time in a continuous gas–liquid process for the hydrochlorination of acetylene, as illustrated in Scheme 1. The catalysts are composed of $AuCl_3$ in 1-propyl-3-methylimidazolium chloride ([Prmim][Cl]) (hereafter referred to as $[Prmim]AuCl_4$) on an activated carbon (AC) support (hereafter referred to as Au–IL/AC). Remarkably, the Au–IL/AC catalyst exhibited a significantly higher catalytic activity (C_2H_2 conversion = 72.1% at 180 °C compared to 16.1% without IL). Moreover, the Au–IL/AC catalyst delivered a stable performance. During 300 h on stream, the C_2H_2 conversion declines only by about 3.7% from the initial 99.4% with the selectivity of VCM reaching more than 99.8%. The main cause of the catalyst deactivation was also studied using ICP, TGA, XPS, TEM and BET analysis. These exciting preliminary results are an indication that Au–IL/AC catalyst represents a highly active and stable catalyst that may replace mercuric chloride.

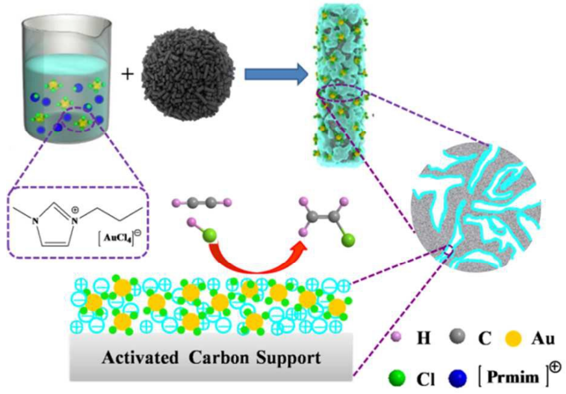

Scheme 1. Schematic view of a supported ionic liquid phase (SILP) catalyst system.

Experimental

Chemicals

Activated carbon (marked as AC, ROX 0.8, pellets of 0.8 mm diameter and 5 mm length) was purchased from NORIT. $HAuCl_4 \cdot 4H_2O$ (the content of Au assay $\geqslant$49%) were purchased from Sigma-Aldrich. The acetylene (gas, 98.0%) was purified by passing it through a $K_2Cr_2O_7$ solution to get rid of H_2S and PH_3, and a H_2SO_4 solution to get rid of H_2O. The acetylene gas then flowed into the catalyst. All the other gases (HCl and N_2) were of ultra high purity (>99.9%) and were used without further purification. The ionic liquid 1-propyl-3-methylimidazolium chloride, [Prmim]Cl (>99%), was procured from Lanzhou Greenchem ILS, LICP. CAS. (Lanzhou, China), and used as received.

Gold ionic liquids synthesis

Gold ionic liquids (1-propyl-3-methylimidazolium tetrachloroaurate ($[Prmim]AuCl_4$)) complex were synthesized by adding [Prmim]Cl to $HAuCl_4 \cdot 4H_2O$ resulting in the rapid formation of a yellow solid, following heating to above its melting points with stirring for 1 h. The nature of the obtained gold ionic liquids was confirmed by XPS (Fig. S1), Raman (Fig. S2), UV-vis (Fig. S3) as well as FTIR (Fig. S4).

Catalyst preparation

Supported Au-IL complex catalyst was prepared using impregnation technique. The Au precursor, $HAuCl_4 \cdot 4H_2O$, and ionic liquid were first dissolved in concentrated hydrochloric acid (36~38%). Then the solution was added dropwise to the pre-treated activated carbon support with agitated stirring. After the solution was homogeneously mixed with the support, the system was subsequently aged at 40 °C for 4 h, followed by air drying at 110 °C for 12 h to finally obtain the catalysts. The as-prepared catalysts were denoted as Au-IL/AC.

Au loading in all the catalysts was fixed at 1000 ppm at various IL loading, namely 5 wt%, 10 wt% and 20 wt%.

Catalyst characterization

BET specific surface areas were measured using N_2 adsorption–desorption isotherms at liquid nitrogen temperature in a Micromeritics ASAP 2000 apparatus for the samples outgassed at 150 °C for 2 h. The KJS method was applied for determining the pore size distribution using the desorption data. XRD measurements of the catalyst samples were performed on a PANalytical-X'Pert PRO generator with Cu Kα radiation (λ=0.1541 nm) that was operated at 60 kV and 55 mA. Diffraction patterns were recorded at a scanning rate of 2 °/min and at a step of 0.02°. TEM analysis was conducted using a transmission electron microscope (TEM, Tecnai G2 F30 S-Twin), operating at an acceleration voltage of 300 keV. The solid samples were finely ground. The resultant fine powders were dispersed ultrasonically in the ethanol and then two drops of the solution were transferred to a carbon/Cu grid (Beijing Zhongjingkeyi Technology Co., Ltd.). Grids were allowed to dry before TEM characterization. The content of metals within the catalyst was analyzed by inductively coupled plasma mass spectroscopy (ICP-MS) with a PerkinElmer Elan DRC-e. Thermogravimetric analysis (TGA) of the samples was performed using a NETZSCH STA 449C Jupiter instrument coupled to a thermal analyzer in an air atmosphere at a flow rate of 30 mL/min. The temperature was increased from 50 to 850 °C at a heating rate of 10 °C/min. FT-IR characterization was carried out on a Fourier transform infrared spectrophotometer (Nicolet 6700, Thermal Fisher Nicolet Corpration, Waltham, America). Thermogravimetric analysis of the solids was performed using a TA instrument (SDT2960 model) by keeping 10–15 mg of the sample under a constant flux of air and using a temperature ramp of 2 °C/min. Raman spectra were obtained by a Nicolet 910 Raman instrument with an inVia Renishaw spectrometer, equipped with a microscope (Nicolet Continum). The excitation wavelength was 785 nm from a Renishaw HPNIR laser with a power of *ca.* 15 mW on the sample.

Activity and selectivity evaluations

The continuous reactor setup used for the SILP catalyzed acetylene hydrochlorination is depicted in Fig. S5. Both acetylene and hydrogen chloride flows were adjusted by means of mass-flow controllers (D07-19B, Beijing Sevenstar Electronic Co., Ltd.). The reactor consisted of a stainless steel tube (10 mm diameter, 400 mm length) equipped with a bronze sinter plate for catalyst placement. A reaction temperature of 180 °C was chosen. Acetylene (5 mL/min, 1 bar) and hydrogen chloride (6 mL/min, 1 bar) were fed though a mixing vessel via calibrated mass flow controllers to a heated glass reactor containing catalyst (0.4 g) with a total GHSV (C_2H_2) of 370 h^{-1}. The long-term stability experiment was performed in the same apparatus under the conditions of 1 g catalyst, GHSV (C_2H_2) of 30 h^{-1}, and the fed volume ratio $V(C_2H_2)/V(HCl)$ of 1:1.2. Blank tests using an empty reactor filled with quartz wool did not reveal any catalytic activity, and quartz sand was used to extend the bed length, above and below the catalyst itself, separated by quartz wool.

The gas phase products were first passed through an absorption bottle containing a NaOH solution to remove excess HCl and then analyzed on-line by gas chromatograph equipped with a flame ionization detector at regular intervals: Injector temperature 150 °C, detector temperature 150 °C, oven temperature 80 °C (isothermal operation). Chromatographic separation and identification of the products was carried out using a Porapak Q packed column (1 m, 3 mm diameter, mesh size 80/100). The composition of the reactor outflow (dissolve in the N-methylpyrrolidone solution) was determined using a Waters GCT Premier chromatograph equipped with a HP-5 capillary column. Product mass fractions were obtained using an internal standard. The main product of acetylene hydrochlorination was vinyl chloride, a small amount of the by-products 1,1-dichloroethane and 1,2-dichlorethane were also produced. The gas-phase products of acetylene hydrochlorination were quantified using the peak area normalization method. Given that hydrogen chloride is absorbed by the absorption liquid after the reaction, the volume of the reaction system can be considered constant during the calculations, and the carbon balance values based on these products are near 100%.The conversion of acetylene and the selectivity to VCM were calculated by Eqs.(1)-(2), as follows:

$$\text{Acetylene conversion }(\%) = \left(1 - \frac{F_A}{F_{A0}}\right) \times 100\% \qquad (1)$$

$$\text{VCM Selectivity }(\%) = \frac{F_{VCM}}{1 - F_A} \times 100\% \qquad (2)$$

Where F_{A0}, F_A, and F_{VCM} represent the volume fraction of acetylene in the raw gas, the volume fraction of remaining acetylene, and the volume fraction of vinyl chloride in the product mixture gas, respectively.

Results and discussion

The catalysts are composed of $AuCl_3$ in 1-propyl-3-methylimidazolium chloride ([Prmim][Cl]) (hereafter referred to as $[Prmim]AuCl_4$) on an activated carbon (AC) support (hereafter referred to as Au–IL/AC). The $[Prmim]AuCl_4$ complex was characterised by X-ray photoelectron spectroscopy (XPS), Raman spectroscopy, UV–vis spectroscopy, and Fourier transform infrared (FTIR) spectroscopy (details of the $[Prmim]AuCl_4$ complex characterization are given in the Supporting Information (Fig. S1–S3)). From these characterisations, we concluded that the square-planar coordination site $AuCl_4^-$ is formed by the reaction of $AuCl_3$ with the chloride anion via an anion-exchange mechanism (Fig. S6), and that metallic Au^0 particles from the reduction of Au^{3+} are not present. FTIR analysis showed that there is a strong interaction between $AuCl_4^-$ and the cationic [Prmim]Cl headgroup (Fig. S4).

AC was chosen as the support for the Au(III)–IL complex system. The Au-IL/AC catalyst was obtained by applying a defined amount of Au(III)–IL complex to the heterogeneous catalyst in concentrated hydrochloric acid, followed by solvent removal and drying. Deposition of Au(III)–IL complex onto the support caused the surface area to decrease from 1135 to 753 m^2/g and the pore volume to decrease from 0.636 to 0.419 cm^3/g, as revealed by Brunauer–Emmett–Teller (BET) measurements. The Au–IL/AC catalyst contained 1000 ppm Au and 10 wt% IL, which corresponds to a theoretical pore-filling degree of 15.86%. Inductively coupled plasma mass spectrometry (ICP-MS) analysis confirmed that Au metal loading was in accordance with the nominal amount of metal impregnated onto the support. X-ray diffraction (XRD) showed that no significant metallic Au crystals were formed in the Au–IL/AC catalyst (Fig. 1a). This is indicative of most of the Au existing as non-crystalline Au^{3+} species or the concentration of Au being too low to be detected by XRD. XPS analysis indicated that more than one gold species was present. Using the known electron binding energies of the various oxidation states of Au, the $4f_{7/2}$ peaks at 84.4 and 87.2 eV were assigned as Au^0 and Au^{3+}, respectively.[2] The ratio of Au^{3+} to Au^0 was 76.09:23.91. The existence of Au^0 species in Au–IL/AC may be because of the reduction of Au^{3+} by carbon, which agrees with previous publications.[2,6,9,42] From scanning transmission electron microscopy (STEM) characterization data, we concluded that most of the Au compounds were homogeneously and highly dispersed on the catalyst materials as non-crystalline Au^{3+} species because there was no evidence of the presence of crystalline NPs. STEM–X-ray energy dispersive spectroscopy (XEDS) mapping (Fig. 1c) and line-scan analysis (Fig. S7) indicated that there was a homogeneous distribution of Au, N, and Cl atoms.

Fig. 2 shows the catalytic performance of the Au–IL/AC catalyst and Au/AC for comparison. Both experiments used the same amount of Au (1000 ppm). Remarkably, Au–IL/AC exhibited significantly higher catalytic activity. As the reaction approached the steady state, Au–IL/AC exhibited >72.1% C_2H_2 conversion (turnover frequency (TOF) = 79.2 h^{-1}. All TOF values were calculated with respect to the total Au content of the catalyst) at C_2H_2 gas hourly space velocity (GHSV) of 370 h^{-1}, which is 4.5 times that of Au/AC. Compared with the wide range of other catalyst materials reported in the literature (Fig. S8), it is clear the Au–IL/AC catalyst is one of the best catalysts reported in terms of TOF. The activity of the Au–IL/AC catalyst is also very close to that state-of-the-art commercial Au/C catalysts at a Au loading of 0.1 wt%,[26] further highlighting the excellent catalytic performance of the material. Note that pure IL/AC was used as a control and showed negligible catalytic activity (< 6% conversion), which excludes the possible contribution of the IL to the hydrochlorination activity. It should be highlighted that for both Au-based catalysts, the selectivity for the formation of VCM was above 99.8% with only trace amounts (< 0.2%) of 1,2-dichloroethane and chlorinated oligomers.

Based on the catalytic results discussed above, Au–IL/AC can be considered to be an efficient catalyst for the hydrochlorination of acetylene. Systematic tests were performed with different amounts of IL. As shown in Fig. 3, the amount of IL affects both the catalyst activity and stability.

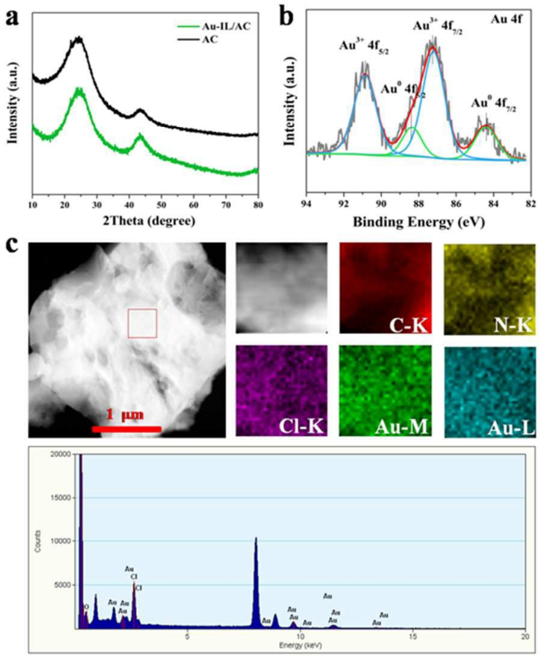

Fig. 1 Characterizations of Au-IL/AC catalyst. (a) XRD patterns of Au-IL/AC and bare AC support. (b) Au 4f XPS spectra of Au-IL/AC catalyst. (c) High-angle annular dark-field image together with the XEDS mapping of Au-IL/AC catalyst.

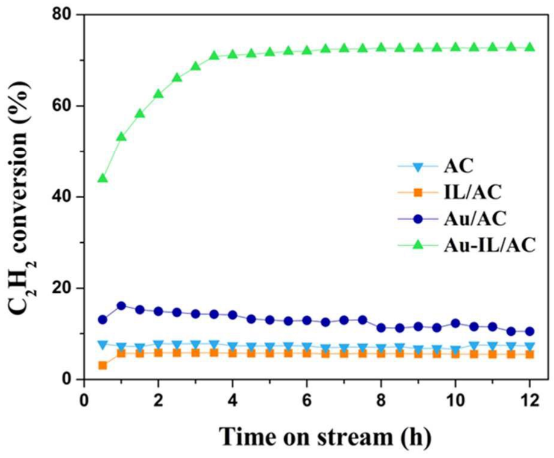

Fig. 2 Conversion of acetylene to VCM in acetylene hydrochlorination over Au-IL/AC, Au/AC, IL/AC and bare AC catalysts. Reaction conditions: T = 180 °C, C_2H_2 gas hourly space velocity (GHSV) = 370 h^{-1}, feed volume ratio $V(HCl)/V(C_2H_2)$ = 1.2.

With increasing amount of IL in the range of 5 to 20 wt%, the maximum conversion decreases from 77.1% to 61.8%. The decrease in activity with increasing IL amount indicates that the IL may interact with the $AuCl_3$ catalyst. To investigate this further, we analysed the surface of the Au–IL/AC catalyst by XPS. The N 1s spectrum confirmed the presence of nitrogen, which must come from the IL because it is the only nitrogen source in the reaction system (Fig. S9). These findings indicate that the IL chemisorbed on the catalyst. The relative N/Au ratio was 0.11% in Au–IL/AC with 5 wt% IL loading, but 0.08%

and 0.05% in Au–IL/AC with 10 wt% IL and Au–IL/AC with 20 wt% IL, respectively (Table 1). The ratio of surface atoms of nitrogen to gold decreasing with increasing IL amount indicates that Au complex ions may be enriched in the top layer of the IL surface. Similar behaviour was also observed by Maier *et al*.[43] Thus, the higher activity with low IL loading (*e.g.*, 5 wt%) can be attributed to a higher concentration of the active Au species at the interface and the generally larger interface area of the solid support. The enrichment of Au complex ions in the top layer of the IL surface may also led to facile agglomeration of Au species during the catalysis processes (Fig. 4), which results in a significant decrease of activity. With increasing IL amount, the catalyst activity decreases because of the dilution effect. That is, the number of Au atoms catalysing the acetylene hydrochlorination is reduced by the high loading of IL because of diffusion of active Au atoms from the top surface layer of the ionic solution to the layers beneath. This is confirmed by the reaction rate decreasing with increasing Au loading (Fig. 5). In the Au loading range from 0.1 to 0.25 wt%, the TOF of the Au–IL/AC system remained constant, indicating that each Au centre has the same activity and no cluster formation occurs (all TOFs were calculated at about 50% C_2H_2 conversion and based on the total Au amount). For Au loading of 0.5 wt%, the observed reaction rate (72.1 h^{-1}) was significantly lower than the reaction rates for Au loading of 0.1 to 0.25 wt% (TOFs between 168.1 and 142.6 h^{-1}). For the range of Au loading between 0.1 and 0.25 wt%, the reaction rate showed a first-order dependence on the Au concentration.

Table 1 Surface composition of Au-IL/AC catalyst with different IL loading, determined by XPS.

Loaded IL amount (wt%)	Au (wt%)	N (wt%)	Au/N ratio (%)
5	0.13	1.19	0.11
10	0.10	1.25	0.08
20	0.07	1.29	0.05

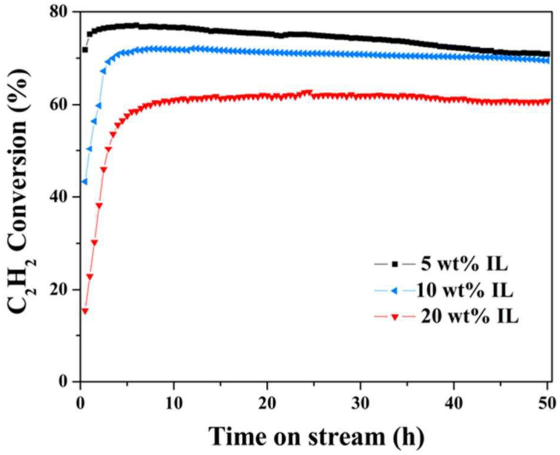

Fig. 3 Catalytic activity of Au-IL/AC as a function of the amount of IL loading. Reaction conditions: T = 180 °C, C_2H_2 gas hourly space velocity (GHSV) = 370 h^{-1}, feed volume ratio $V(HCl)/V(C_2H_2)$ = 1.2.

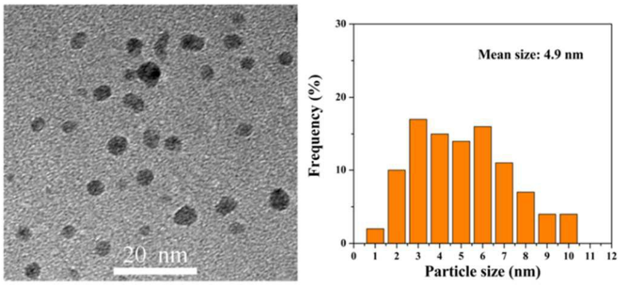

Fig. 4 Representative STEM figure of used Au-IL/AC with 5 wt% IL loading and corresponding particle size distributions.

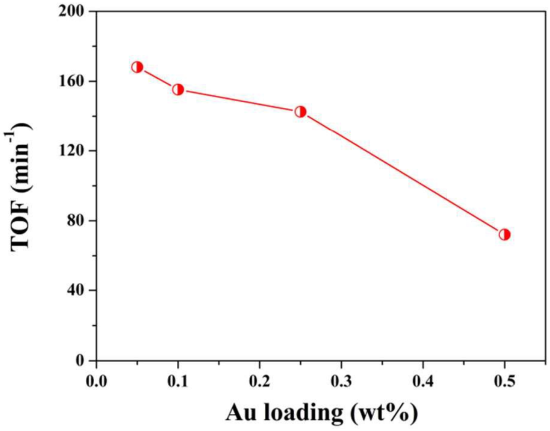

Fig. 5 Catalytic activity of Au-IL/AC as a function of the amount of Au loading. Reaction conditions: T = 180 °C, C_2H_2 gas hourly space velocity (GHSV) = 370 h^{-1}, feed volume ratio $V(HCl)/V(C_2H_2)$ = 1.2.

Table 2 Pore volume and surface area related to the IL loading as measured by N_2-physisorption.

Loaded IL amount (wt%)	S_{BET} (m^2/g)	V_{tot} (cm^3/g)[a]	V_{IL} (cm^3/g)[b]	V_{na} (cm^3/g)[c]	V_{BP} (cm^3/g)[d]	αIL (%)[e]
0	1135	0.636	/	/	/	/
5	966	0.521	0.045	0.083	0.038	7.51
10	753	0.419	0.091	0.153	0.062	15.86
20	148	0.084	0.182	0.425	0.243	35.69

[a] Total pore volume, determined by the amount adsorbed at P/P_0 = 0.99 in the N_2 adsorption isotherm at -196 °C.

[b] Amount of IL in samples IL/AC.

[c] Pore volume not accessible to N_2 determined as total pore volume of support AC minus total pore volume of sample IL/AC.

[d] Blocked porosity volume.

[e] Theoretical pore-filling degree.

In addition, the degree of pore-filling decreased from 7.51% to 35.69% with increasing IL loading from 5 to 20 wt% (Table 2). This may also have a significant effect on the activity of the three catalysts. The decreasing activity with increasing IL loading is most likely a result of the longer residence time of the reactant gas in the SILP system or part of the pore volume not being accessible to the substrate (the blocked porosity also increased from 0.038 to 0.243 cm^3/g with increasing IL loading). Palomar et al. previously suggested the presence of blocked

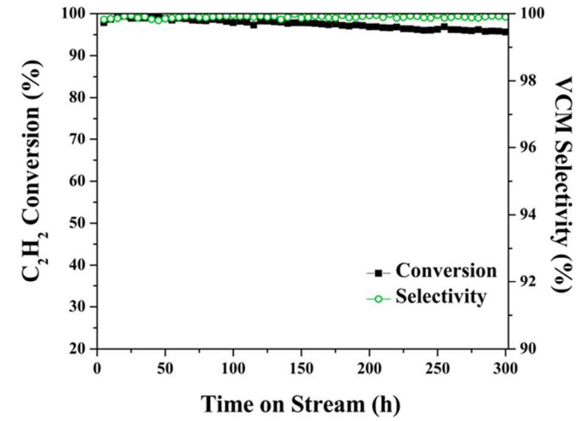

Fig. 6 Long-term stability test of Au-IL/AC catalyst. Reaction conditions: T = 180 °C, C_2H_2 gas hourly space velocity (GHSV) = 30 h^{-1}, feed volume ratio $V(HCl)/V(C_2H_2)$ = 1.2.

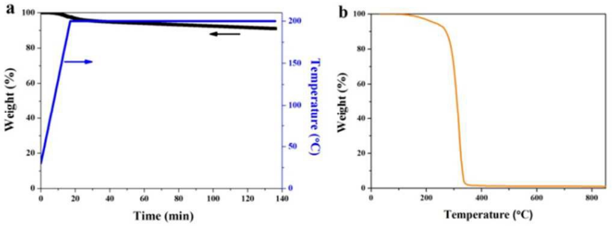

Fig. 7 (a) TGA of Au-IL/AC: initial temperature ramp of 10 °C/min to 200 °C, where the temperature is kept constant for 2 h. (b) TGA of [Prmim]Cl.

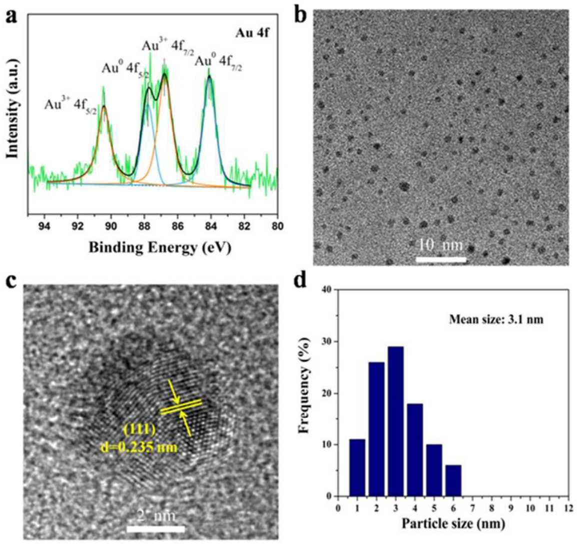

Fig. 8 Structure characterization of the used Au-IL/AC catalyst. (a) XPS spectra. a.u.: arbitrary units. (b) TEM image. (c) HRTEM image. (d) Au particle size distribution.

porosity in the case of IL adsorbed on a commercial AC.[44] Thus, the IL layer decreases the availability of the substrate at the active sites because the high viscosity IL may induce mass transfer limitations or the access of gases to some porosity is impeded by pore blockage. However, both of these have only a minor influence on the IL and transition metal catalyst taking part in the catalysed reaction.

To demonstrate the long-term stability of the developed acetylene hydrochlorination catalyst, we used the Au–IL SILP system for more than 300 h time-on-stream (Fig. 6). The acetylene conversion decreased by only about 3.7% from the initial conversion of 99.4%, indicating that Au–IL/AC maintains its high activity under industrial operation conditions. [Prmim]Cl IL is suitable for such long-term testing because this IL is thermally stable under the reaction conditions (Fig. 7a) and thermal decomposition occurs at more than 280 °C (Fig. 7b). XPS analysis of the catalyst before and after its use in the acetylene conversion reaction also indicated that IL leaching was negligible, with no considerable change in the N/C atomic ratio (2.63% vs. 2.41%). ICP-MS analysis of the Au–IL/AC catalyst after the reaction also did not reveal significant Au loss during the reaction (detection limit *ca.* 100 ppb).

To further understand the reasons for the catalyst deactivation, XPS, TEM, BET analysis was employed. XPS analysis showed that the ratio of Au^{3+} to Au^0 after the reaction was 53.48:46.52 (Fig. 8a). Previous literature studies ascribed the activity of the Au based catalyst to the presence of Au^{3+} species postulating them as active sites. These results demonstrate that even the Au^{3+} species are relative stable in the presence of IL even after 300 h under high temperature, a fraction of Au^{3+} species still tend to reduction during the catalysis processes which results in a significant decrease of activity. The stable presence of Au^{3+} can be attributed to the electric potential of $AuCl_4^-$ ($AuCl_4^-/Au^0$ = 0.926 V) being significantly lower than that of Au^{3+} (Au^{3+}/Au^0 = 1.52 V), and therefore the reduction rate of Au^{3+} to Au^0 by C_2H_2 is significantly lower. Thus, the role of IL in promoting the activity of Au is to stabilise the formation of Au^{3+}. Using dark-field transmission electron microscopy (TEM), the visible particles were identified as Au NPs in the TEM–XEDS images (Fig. S10). Au NPs with a mean size of about 3.1 nm were evenly distributed throughout the supporting material (Fig. 8b and 8d). Au NPs with well-defined lattice fringes in the high-resolution TEM image confirmed the (111) crystal plane of Au, because the crystal plane spacing was measured as 0.235 nm (Fig. 8c). Although some very small Au particles were observed after 300 h, clusters/aggregations of Au^0 were not observed during the reaction. This is understandable because ILs have been found to be very good media for generating highly dispersed Au NPs without extra stabilising molecules, and very small Au NPs can be synthesized in various ILs (*e.g.*, $BmimBF_4$, BmimCl, and $BmimPF_6$) by chemical reduction.[45-55] The ILs initially form a protective layer around Au ions, and weakly coordinating ions will bind to NP surfaces to give a classic ion-based Derjaguin–Landau–Verwey–Overbeek-type Coulombic repulsion via both electronic and steric protection of Au NPs.[56] Au^{3+} is reduced to Au^0 during the reaction; however, carbon deposition may also result in pore clogging of the support and covering some parts of the active sites and decreasing the catalyst activity. Thus, to provide direct evidence of coke deposition, BET experiments were performed. After the 300 h running, the surface area and pore volume obtained by N_2-physisorption are 769 m^2/g and 0.420 cm^3/g, respectively. No drastic changes in the textural properties of the materials were observed when compared with that of the fresh Au-IL/AC catalyst. It can be concluded that less coke is therefore deposited on this catalyst. Considering that the active component is indeed developed in a homogeneous reaction medium in Au-IL/AC catalyst, it is reasonable that the disadvantages of a gas-solid reaction, such as the carbon deposition and the regional hot-spot, could be overcome, as reported by Cao *et al*.[57]

Previous studies have demonstrated that AC plays an important role in the performance of Au-based catalysts because surface oxygenated groups on the AC surface are the key components governing the unique catalytic activity and stability of the Au^{3+} catalyst.[23] However, AC is easily crushed under reaction conditions, resulting in loss of the active species and deactivation of the catalyst. Therefore, efforts are ongoing to replace carbon supports. We were also interested in whether the observed principles could be applied to more common heterogeneous catalysts, which additionally allows the IL effect to be studied in a more general manner. Further experiments were performed to investigate the possibility of immobilising Au(III)–IL complexes on oxide (*e.g.*, TiO_2, SiO_2, or Al_2O_3) and zeolite (*e.g.*, ZSM-5) supports (Table 3). The results confirmed that SILP materials based on the Au(III)–IL complex can be used with other porous supports, demonstrating the feasibility of other porous supports as a substitute for the AC support. Despite the slower conversion compared with the AC-supported Au-based catalysts, the catalysts were superior to their IL-free counterparts (comparative experiments with the IL-free solid catalysts based on TiO_2, SiO_2, Al_2O_3 and ZSM-5 showed nearly no conversion for the hydrochlorination of acetylene under the same conditions). The lower activity of oxide- and zeolite-supported Au-SILP systems is most likely because of the lower BET surface area, and thus the smaller interface area of the solid support, compared with AC. In addition, the important role of the surface chemistry may affect the catalytic performance of Au-SILP catalysts. This will be investigated in future work.

Table 3 Hydrochlorination of acetylene with Au-SILP catalysts with different supports.[a]

Support	S_{BET} (m^2/g)	V_{tot} (cm^3/g)	Con. (%)	Sel. (%)
TiO_2 (P25)	49	0.12	12.7	99.6%
SiO_2	370	0.92	17.6	99.8%
Al_2O_3	263	0.63	22.6	99.7%
ZSM-5 (Si/Al=360)	321	0.28	32.1	> 99.9%

[a] Reaction conditions: 180 °C, 1 bar, 1000 ppm Au, αIL (pore-filling degree) = 15%, GHSV(C_2H_2) = 370 h^{-1}, feed volume ratio V(HCl)/V(C_2H_2) = 1.2.

Conclusion

In conclusion, we have demonstrated a synthetically straight-forward, highly effective way to drastically enhance the activity and stability of heterogeneous Au based catalyst in the acetylene hydrochlorination reaction. It demonstrated that stable and catalytically active Au(III) complexes can be obtained using SILP technology. The resulting heterogeneous Au–IL/AC catalysts combine the advantages of the catalytic species being stabilised in the Au(III) form by forming a Au(III)–IL complex and the need for less expensive metal catalyst because the active component can be better developed in a homogeneous reaction medium. The Au–IL/AC catalyst system gives much higher catalytic performance in catalysed acetylene hydrochlorination compared with the IL-free Au/AC catalyst and a wide range of other catalyst materials reported in the literature. The long-term stability of the developed systems is remarkably high, indicating the potential of these SILP catalysts in industrial VCM production.

Acknowledgements

The financial support by the National Natural Science Foundation of China (NSFC-21476207) is gratefully acknowledged.

References

1 H. Schobert, *Chem. Rev.*, 2014, **114**, 1743-1760.
2 M. Conte, C. J. Davies, D. J. Morgan, T. E. Davies, D. J. Elias, A. F. Carley, P. Johnston, G. J. Hutchings, *J. Catal.*, 2013, **297**, 128-136.
3 R. J. Tedeschi, *Chemical Industries, Vol. 6*, Marcel Dekker, Inc., 1982.
4 G. J. Hutchings, *J. Catal.*, 1985, **96**, 292-295.
5 B. Nkosi, N. J. Coville, G. J. Hutchings, *J. Chem. Soc., Chem. Commun.*, 1988, **1**, 71-72.
6 M. Conte, C. J. Davies, D. J. Morgan, T. E. Davies, A. F. Carley, P. Johnston, G. J. Hutchings, *Catal. Sci. Technol.*, 2013, **3**, 128-134.
7 B. Nkosi, N. J. Coville, G. J. Hutchings, M. D. Adams, J. Friedl, F. E. Wagner, *J. Catal.*, 1991, **128**, 366-377.
8 J. Zhang, Z. He, W. Li, Y. Han, *RSC Adv.*, 2012, **2**, 4814-4821.
9 M. Conte, C. J. Davies, D. J. Morgan, A. F. Carley, P. Johnston, G. J. Hutchings, *Catal. Lett.*, 2014, **144**, 1-8.
10 M. Conte, A. F. Carley, G. Attard, A. A. Herzing, C. J. Kiely, G. J. Hutchings, *J. Catal.*, 2009, **266**, 164.
11 W. Wittanadecha, N. Laosiripojana, A. Ketcong, N. Ningnuek, P. Praserthdam, J. R. Monnier, S. Assabumrungrat, *Appl. Catal. A: Gen.*, 2014, **475**, 292-296.
12 X. Yang, C. Jiang, Z. Yang, J. Zhang, *J. Mater. Sci. Technol.*, 2014, **30**, 434-440.
13 H. Zhang, B. Dai, X. Wang, L. Xu, M. Zhu, *J. Ind. Eng. Chem.*, 2012, **18**, 49-54.
14 H. Zhang, B. Dai, X. Wang, W. Li, Y. Han, J. Gu, J. Zhang, *Green Chem.*, 2013, **15**, 829-836.
15 Y. Pu, J. Zhang, X. Wang, H. Zhang, L. Yu, Y. Dong, W. Li, *Catal. Sci. Technol.*, 2014, **4**, 4426-4432.
16 H. Zhang, W. Li, X. Li, W. Zhao, J. Gu, X. Qi, Y. Dong, B. Dai, J. Zhang, *Catal. Sci. Technol.*, 2015, **5**, 1870-1877.
17 J. Zhao, J. Xu, J. Xu, J. Ni, T. Zhang, X. Xu, X. Li, *ChemPlusChem*, 2015, **80**, 196-201.

18 H. Zhang, B. Dai, W. Li, X. Wang, J. Zhang, M. Zhu, J. Gu, *J. Catal.*, 2014, **316**, 141-148.
19 J. Zhao, T. Zhang, X. Di, J. Xu, S. Gu, Q. Zhang, J. Ni, X. Li, *Catal. Sci. Technol.*, 2015, **5**, 4973-4984.
20 K. Zhou, J. Jia, X. Li, X. Pang, C. Li, J. Zhou, G. Luo, F. Wei, *Fuel Process. Technol.*, 2013, **108**, 12-18.
21 J. Xu, J. Zhao, T. Zhang, X. Di, S. Gu, J. Ni, X. Li, *RSC Adv.*, 2015, **5**, 38159-38163.
22 K. Zhou, J. Si, J. Jia, J. Huang, J. Zhou, G. Luo, F. Wei, *RSC Adv.*, 2014, **4**, 7766-7769.
23 X. Li, X. Pan, L. Yu, P. Ren, X. Wu, L. Sun, F. Jiao, X. Bao, *Nat. Commun.*, 2014, 5, 3688-3694.
24 X. Li, Y. Wang, L. Kang, M. Zhu, B. Dai, *J. Catal.*, 2014, **311**, 288-294.
25 K. Zhou, B. Li, Q. Zhang, J. Q. Huang, G. L. Tian, J. C. Jia, M. Q. Zhao, G. H. Luo, D. S. Su, F. Wei, *ChemSusChem*, 2014, **7**, 723-728.
26 P. Johnson, N. Carthey, G. J. Hutchings, *J. Am. Chem. Soc.*, 2015, **137**, 14548-14557.
27 C. P. Mehnert, R. A. Cook, N. C. Dispenziere, M. Afeworki, *J. Am. Chem. Soc.*, 2002, **124**, 12932-12933.
28 A. Riisager, K. M. Eriksen, P. Wasserscheid, R. Fehrmann, *Catal. Lett.*, 2003, **90**, 149-153.
29 C. P. Mehnert, E. J. Mozeleski, R. A. Cook, *Chem. Commun.*, 2002, **24**, 3010-3011.
30 S. Breitenlechner, M. Fleck, T. E. Müller, A. Suppan, *J. Mol. Catal. A: Chem.*, 2004, **214**, 175-179.
31 M. Haumann, K. Dentler, J. Joni, A. Riisager, P. Wasserscheid, *Adv. Synth. Catal.*, 2007, **349**, 425-431.
32 A. Riisager, P. Wasserscheid, R. Van Hal, R. Fehrmann, *J. Catal.*, 2003, **219**, 452-455.
33 M. J. Schneider, M. Lijewski, R. Woelfel, M. Haumann, P. Wasserscheid, *Angew. Chem., Int. Ed.*, 2013, **52**, 6996-6999.
34 U. Hintermair, T. Hoefener, T. Pullmann, G. Francio, W. Leitner, *ChemCatChem*, 2010, **2**, 150-154.
35 M. Jakuttis, A. Schoenweiz, S. Werner, R. Franke, K. D. Wiese, M. Haumann, P. Wasserscheid, *Angew. Chem., Int. Ed.*, 2011, **50**, 4492-4495, S4492/4491-S4492/4494.
36 F. Schwab, M. Lucas, P. Claus, *Angew. Chem., Int. Ed.*, 2011, **50**, 10453-10456, S10453/10451-S10453/10455.
37 A. Riisager, R. Fehrmann, S. Flicker, R. van Hal, M. Haumann, P. Wasserscheid, *Angew. Chem., Int. Ed.*, 2005, **44**, 815-819.
38 S. Xun, W. Zhu, D. Zheng, H. Li, W. Jiang, M. Zhang, Y. Qin, Z. Zhao, H. Li, *RSC Adv.*, 2015, **5**, 43528-43536.
39 M. Armand, F. Endres, D. R. MacFarlane, H. Ohno, B. Scrosati, *Nat. Mater.*, 2009, **8**, 621-629.
40 L. F. Bobadilla, T. Blasco, J. A. Odriozola, *Phys. Chem. Chem. Phys.*, 2013, **15**, 16927-16934.
41 M. H. Valkenberg, C. deCastro, W. F. Holderich, *Green Chem.*, 2002, **4**, 88-93.
42 J. Zhao, J. Xu, J. Xu, T. Zhang, X. Di, J. Ni, X. Li, *Chem. Eng. J.*, 2015, **262**, 1152-1160.
43 F. Maier, J. M. Gottfried, J. Rossa, D. Gerhard, P. S. Schulz, W. Schwieger, P. Wasserscheid, H. P. Steinrueck, *Angew. Chem., Int. Ed.*, 2006, **45**, 7778-7780.
44 J. Palomar, J. Lemus, M. A. Gilarranz, J. J. Rodriguez, *Carbon*, 2009, **47**, 1846-1856.
45 L. S. Ott, R. G. Finke, *Coord. Chem. Rev.*, 2007, **251**, 1075-1100.
46 K. S. Kim, D. Demberelnyamba, H. Lee, *Langmuir*, 2004, **20**, 556-560.
47 H. Itoh, K. Naka, Y. Chujo, *J. Am. Chem. Soc.*, 2004, **126**, 3026-3027.
48 J. Vignolle, T. D. Tilley, *Chem. Commun.*, 2009, **46**, 7230-7232.
49 M. Hasan, I. V. Kozhevnikov, M. R. H. Siddiqui, A. Steiner, N. Winterton, *Inorg. Chem.*, 1999, **38**, 5637-5641.
50 R. Tatumi, H. Fujihara, *Chem. Commun.*, 2005, **(1)**, 83-85.
51 D. M. Stefanescu, D. S. Glueck, R. Siegel, R. E. Wasylishen, *Langmuir*, 2004, **20**, 10379-10381)
52 H. S. Schrekker, M. A. Gelesky, M. P. Stracke, C. M. L. Schrekker, G. Machado, S. R. Teixeira, J. C. Rubim, J. Dupont, *J. Colloid. Interf. Sci.*, 2007, **316**, 189-195.
53 J. Huang, T. Jiang, H. Gao, B. Han, Z. Liu, W. Wu, Y. Chang, G. Zhao, *Angew. Chem., Int. Ed.*, 2004, **43**, 1397-1399.
54 S. Tang, G. A. Baker, H. Zhao, *Chem. Soc. Rev.*, 2012, **41**, 4030-4066.
55 I. Dolamic, S. Knoppe, A. Dass, T. Burgi, *Nat. Commun.*, 2012, **3**, 798-803.
56 P. Zhang, Z. A. Qiao, X. Jiang, G. M. Veith, S. Dai, *Nano Lett.*, 2015, **15**, 823-828.
57 G. Qin, Y. Song, R. Jin, J. Shi, Z. Yu, S. Cao, *Green Chem.*, 2011, **13**, 1495-1498.

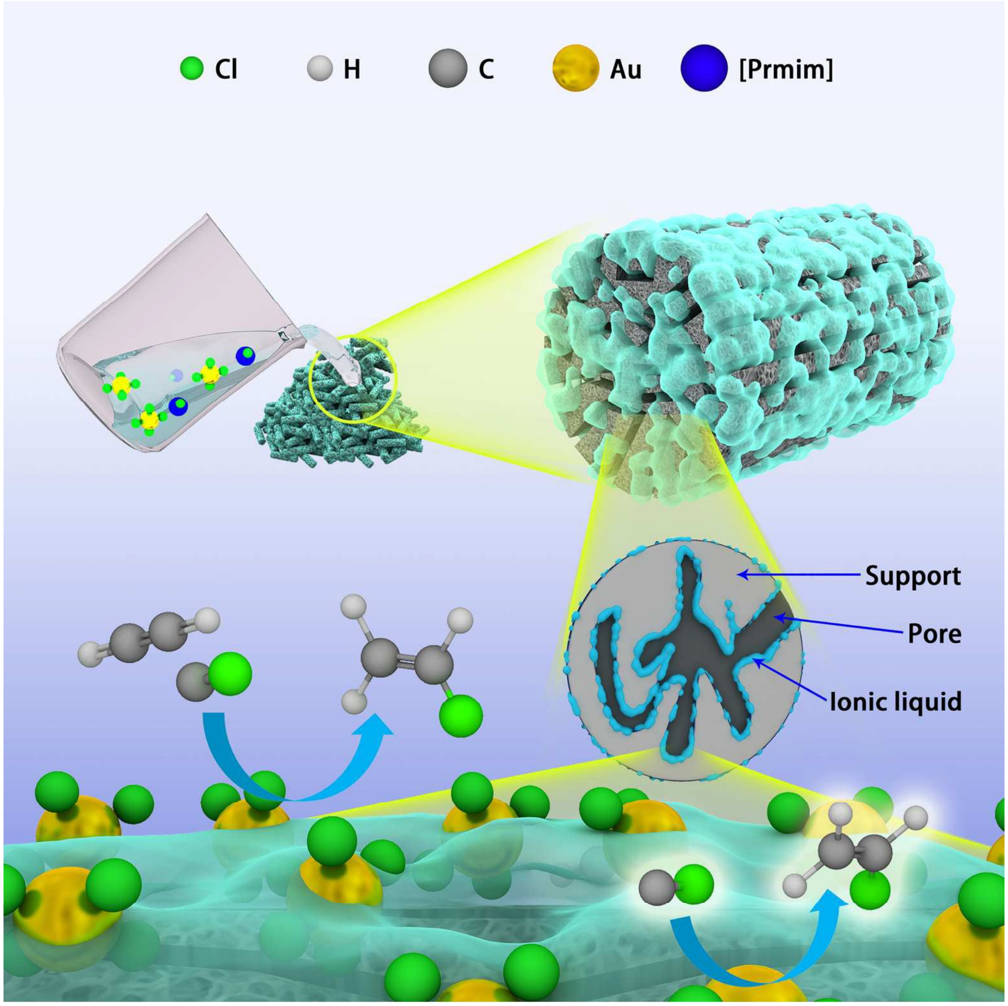

160x160mm (300 x 300 DPI)